Discontinuity, Nonlinearity, and Complexity 7(1) (2018) 67-79

Discontinuity, Nonlinearity, and Complexity

https://lhscientificpublishing.com/Journals/DNC-Default.aspx

Evolution Towards the Steady State in a Hopf Bifurcation: A Scaling Investigation

Vinícius B. da Silva†, Edson D. Leonel

Departamento de Física, UNESP - Univ Estadual Paulista, Av. 24A, 1515 - Bela Vista, 13506-900, Rio Claro, SP, BRA

Submission Info

Communicated by V. Afaimovich
Received 30 January 2017
Accepted 13 April 2017
Available online 1 April 2018

Keywords

Hopf bifurcation
Scaling properties
Critical exponents
Normal forms

Abstract

Some scaling properties describing the convergence for the steady state in a Hopf bifurcation are discussed. Two different procedures are considered in the investigation: (i) a phenomenological description obtained from time series coming from the numerical integration of the system, leading to a set of critical exponents and hence to scaling laws; (ii) a direct solution of the differential equations, which is possible only in the normal form. At the bifurcation, the convergence to the stationary state obeys a generalized and homogeneous function. For short time, the dynamics giving by the distance from the fixed point is mostly constant when a critical time is reached hence changing the dynamics to a convergence for the steady state given by a power law. Both the size of the constant plateau and the characteristic crossover time depend on the initial distance from the fixed point. Near the bifurcation, the convergence is described by an exponential decay with a relaxation time given by a power law.

1 Introduction

In general, the dependence on one or more parameters characterizes most of the dynamical systems. In the simple harmonic oscillator, the natural frequency of oscillation is an example of such parameter. The parameter variation may change the qualitative structure of the flow of solutions related to a dissipative dynamical system therefore changing the topological solution of a given attractor. A bifurcation is the name given to the qualitative change in the dynamics [1] due to a parameter variation. Bifurcations are observed in a variety of systems including dynamical population [2, 3], electric circuits [4, 5], chemical reactions [6, 7], discrete mappings [8, 9], laser [10–12] and many others [13–15].

There are two different classes of bifurcations: (i) local and; (ii) global. In a local bifurcation the variation of a control parameter produces a change of stability of a fixed point, indeed an attractor, and hence the topological modifications in the system can be confirmed by an investigation near the fixed point, therefore a local analysis. For a global bifurcation, invariant structures collide with each other and this include a collision between an invariant manifold and chaotic attractor, yielding in a destruction of the chaotic attractor. As a consequence, a major change in the global topology of the system can not be foreseen by a local analysis of fixed point.

†Corresponding author.
Email address: viniciusx10@yahoo.com.br

ISSN 2164-6376, eISSN 2164-6414/$-see front materials
DOI:10.5890/DNC.2018.03.006

In this class of bifurcation lives the so called crisis events [16–19]. We concentrate in a special type of local bifurcation, namely Hopf bifurcation. The achievement of the stationary state of a dissipative system, in many cases, leads to attractors in the phase space. Such attractors might be of zero dimension, *id est* fixed points, or one-dimensional - limit cycles - or higher dimension attractors. The eigenvalues of the Jacobian matrix for the dynamical equations of the system, while evaluated at the attractors, give their stability. The attractor is reached while an initial condition is given along the basin of attraction of an attractor and evolved for a sufficient long time, therefore an asymptotic dynamics. By asymptotic, one understands as long enough time such as $t \to \infty$.

However a clear discussion regarding the dynamics evolving towards the attractor and its corresponding scaling properties were, so far, not made. Our attempt here is to fill up this gap. Therefore, the main goal of this work is to explore the evolution towards the steady state at and near at a Hopf bifurcation. We focus particularly in its normal form. To do so we shall apply a scaling formalism like the one used in statistical mechanics [20,21] to describe phase transitions [22–24]. We consider a dynamical system described by a set of ordinary differential equations written in the so-called normal form. It mimics the dynamics of a complex system however keeping only the lowest nonlinear terms as possible to reproduce the phenomenon. This implies that a complicated set of equations can be expanded in Taylor series and that the normal form reproduces all the dynamics of such set of equations near the criticality.

Before the bifurcation, the dynamics converges to a fixed point which is asymptotically stable. At the bifurcation, the fixed point loses stability and after the bifurcation it repeals the dynamics which converges to a closed orbit in a plane, indeed a limit cycle. Because the attractor is a closed cycle in a plane, it turns out that the polar coordinates is the most convenient set of variables to describe the dynamics, hence the dynamics is obtained by the radius, ρ, and angle ϕ. At the bifurcation, we notice the following: given an initial condition close to the fixed point and inside of the basin of attraction of the fixed point, the dynamical variable ρ keeps almost constant in a long plateau until it suffers a changeover marked by a characteristic crossover time and decays to the fixed point with a behavior described by a power law. The size of the plateau depends on the initial distance from the fixed point as so the crossover time. This type of dynamics obeys a generalized and homogeneous function that leads to a set of three critical exponents yielding also in a scaling law. Near the bifurcation, the dynamics is no longer described by a homogeneous function, but rather by an exponential decay. The relaxation time is given by a power law whose argument corresponds to the distance, in the parameter, to where the bifurcation happened.

This paper is organized as follows. In Section 2 we discuss the normal form of Hopf bifurcation. Section 3 is devoted to describe a phenomenological approach based on a set of three scaling hypotheses leading to critical exponents and hence to a scaling law. In Section 4 we dedicate to investigate an analytical description of the convergence to the steady state in the Hopf bifurcation confirming the results obtained by numerical simulation. Discussions and conclusions are made in Section 5.

2 The normal form of the Hopf Bifurcation

A set of differential equations that describes a Hopf bifurcation [1] is written as

$$\dot{x} = x\mu - w_0 y + (ax - by)(x^2 + y^2) + O(5), \tag{1}$$

$$\dot{y} = y\mu + w_0 x + (ay + bx)(x^2 + y^2) + O(5), \tag{2}$$

where x and y are dynamical variables, μ is a control parameter, a, b and w_0 are constants. Here the term $O(5)$ represents the higher-order term of the type x^{k_1} and y^{k_2} with $k_1 + k_2 = 5$. The following lemma is proved in Appendix this paper.

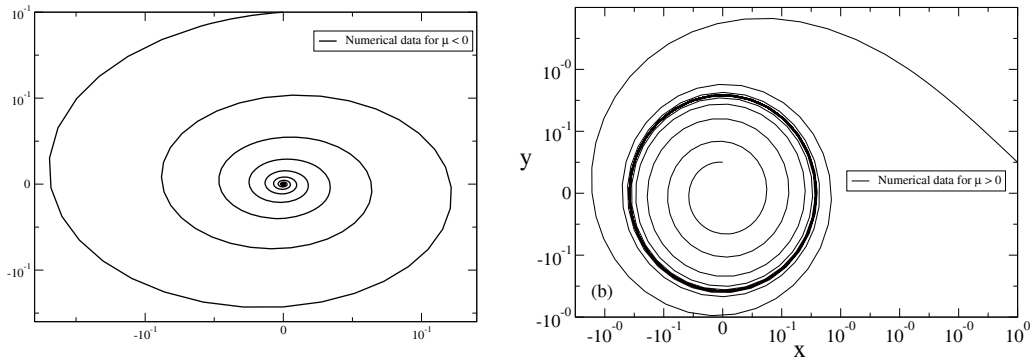

Fig. 1 Phase portraits for y *vs*. x for values of μ: (a) before and, (b) after the bifurcation, respectively.

Theorem 1. *The system described by equations (1) and (2) is locally topologically equivalent near the origin to system described by equations (3) and (4).*

$$\dot{x} = x\mu - w_0 y + (ax - by)(x^2 + y^2), \tag{3}$$

$$\dot{y} = y\mu + w_0 x + (ay + bx)(x^2 + y^2). \tag{4}$$

Therefore, the higher-order terms in the set of equations do not interfere in the bifurcation behavior of the system.

Since after the bifurcation the dynamics lives in a plane, it is convenient to use polar coordinates instead of rectangular variables. Fixing $w_0 = 1$ and $a = -1$, equations (3) and (4) can be written in polar coordinates as

$$\frac{d\rho}{dt} = \mu\rho - \rho^3, \tag{5}$$

$$\frac{d\phi}{dt} = 1 + b\rho^2, \tag{6}$$

where ρ and ϕ describe the radial and the angular coordinates, respectively. Besides that, μ controls the stability of the fixed point at the origin, w_0 gives the frequency of infinitesimal oscillations, and b is a free parameter. In the next section we discuss the scaling properties of dynamics at a Hopf bifurcation.

3 A phenomenological description and scaling properties

We discuss now a phenomenological approach to explore the evolution towards the steady state at and near at a Hopf bifurcation. As we could see in the previous section, the set of equations (5) and (6) are characterized by radial and angular variables. However, to explore the scaling properties that characterize the bifurcation, the equations are analyzed separately. We start first with the radial equation.

The fixed points are obtained by solving $f(\rho) = \mu\rho - \rho^3 = 0$. The solutions have physical meaning only when $\rho \geq 0$. We therefore end up with two fixed points $\rho_1^* = 0$, and $\rho_2^* = \sqrt{\mu}$. As we can see in Figure 1, when $\mu < 0$ the origin $\rho_1^* = 0$ becomes a stable spiral whose sense of rotation depends on the sign of w_0. For $\mu = 0$ the origin is still a stable spiral however the speed of convergence is different from $\mu < 0$. Finally, for $\mu > 0$ there is an unstable spiral at the origin and a stable circular limit cycle at $\rho_2^* = \sqrt{\mu}$, as discussed in [1].

The natural variable to describe the decay to the steady state is the distance from the fixed point [25]. So, for the fixed point $\rho_1^* = 0$ the distance taken from the stationary state is the own dynamical variable $\rho(t)$. The decay to the steady state must also depend of the time t, the initial condition ρ_0, and the parameter μ. Since $\mu = 0$ defines the bifurcation, the convergence to the fixed point is shown in Figure 2 for different initial conditions of ρ_0.

We see from Figure 2 that depending on the initial condition ρ_0, the dynamics stays in a constant plateau for different intervals of time until eventually reaching a characteristic crossover time, t_x, and the orbit changes

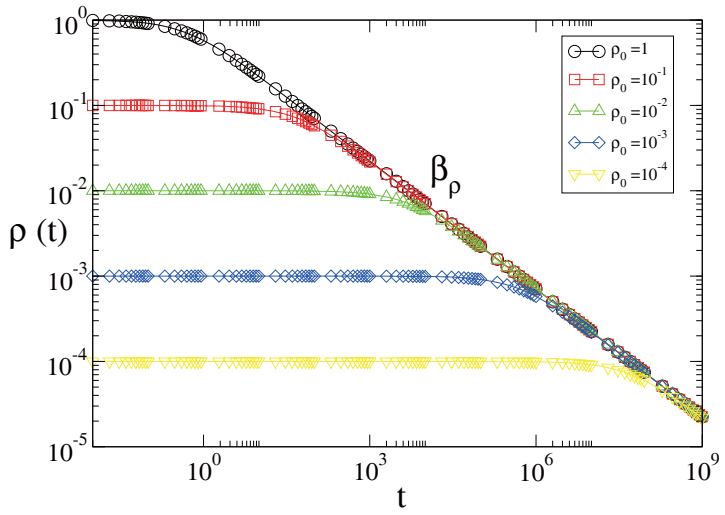

Fig. 2 Convergence to the steady state at $\rho_1^* = 0$ for different initial conditions as shown in the figure. The parameter used was $\mu = 0$ and the differential equations (5) and (6) were numerical integrated using a 4th order Runge-Kutta algorithm. We chose also $w_0 = 1.0$ and $b = 1.0$.

from a constant regime to a power law decay given by a critical exponent β_ρ. We notice that the length of the plateau shows a clear dependence on the initial condition ρ_0. Based on the behavior observed from Figure 2, we can propose the following scale hypotheses:

1. For a short interval of time t, say $t \ll t_x$, the convergence to the steady state is given by

$$\rho(t) \propto \rho_0^{\alpha_\rho}, \quad t \ll t_x. \tag{7}$$

   A quick analysis of Figure 2 allows us to conclude that $\alpha_\rho = 1$.

2. For a sufficient large t, say $t \gg t_x$, the convergence to the steady state is given by

$$\rho(t) \propto t^{\beta_\rho}, \quad t \gg t_x, \tag{8}$$

   where β_ρ gives the decay exponent.

3. The characteristic crossover time t_x that describes the changeover from a constant regime to a power law decay is given by

$$t_x \propto {\rho_0}^{z_\rho}, \tag{9}$$

   where z_ρ is called as the changeover exponent.

The exponents z_ρ and β_ρ are obtained by their specific plots. After the constant plateau, a power law fitting gives $\beta_\rho = -0.499(3) \simeq -0.5$. To obtain the exponent z_ρ we need to analyze the behavior of t_x *vs.* ρ_0, as shown in Figure 3. The slope obtained for t_ρ *vs.* ρ_0 is $z_\rho = -2.00360(6) \simeq -2$.

Based on the behavior shown in Figure 2 and considering the three scaling hypotheses, it is possible to describe the behavior of ρ as a homogeneous and generalized function of the variables t and ρ_0, when $\mu = 0$, as

$$\rho(\rho_0, t) = \ell \rho(\ell^c \rho_0, \ell^d t), \tag{10}$$

where ℓ is a scaling factor, c and d are characteristic exponents. As ℓ is a scaling factor, we chose $\ell^c \rho_0 = 1$, therefore leading to $\ell = \rho_0^{-1/c}$. By substituting this expression in equation (10) we end up with

$$\rho(\rho_0, t) = \rho_0^{-1/c} \rho(1, \rho_0^{-d/c} t). \tag{11}$$

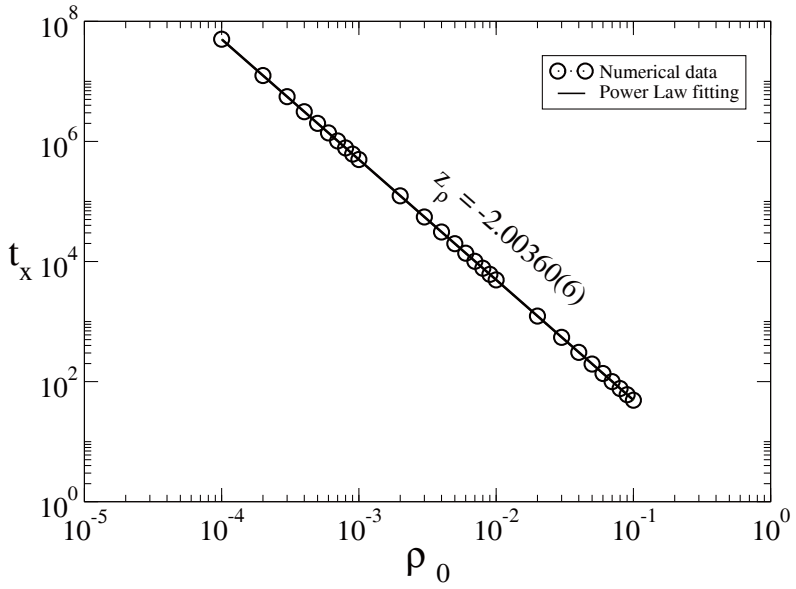

Fig. 3 Plot of the crossover time t_x against the initial condition ρ_0 together with its power law fitting giving $z_\rho = -2.00360(6)$.

We assume $\rho(1,\rho_0^{-d/c}t)$ as a constant for $t \ll t_x$. Comparing equation (11) with the first scaling hypothesis we conclude that $\alpha_\rho = -1/c$.

We now chose $\ell^c\rho_0 = 1$ yielding $\ell = t^{-1/c}$. Substituting in equation (10) we obtain for $t \gg t_x$ that

$$\rho(\rho_0,t) \propto t^{-1/d}. \tag{12}$$

A direct comparison of this result with the second scaling hypothesis gives $\beta_\rho = -1/d$. Finally, by comparing the two expressions obtained for the scaling factor ℓ we arrive in $t_x = \rho_0^{\alpha_\rho/\beta_\rho}$. A comparison with the third scaling hypothesis allows us to obtain the following scaling law

$$z_\rho = \alpha_\rho/\beta_\rho. \tag{13}$$

The knowledge of any two exponents allows determining the third one by substituting equation (13). Besides that, the exponents can also be used to rescale the variables $\rho(t)$ and t in a convenient way such that $\rho \to \rho/\rho_0^{\alpha_\rho}$ and $t \to t/\rho_0^{z_\rho}$ and overlap all curves of $\rho(t)$ *vs.* t shown in Fig. 2 onto a single and hence universal curve, as shown in Figure 4.

Once we have discussed the convergence to the steady state at the bifurcation point, we now discuss the dynamics for $\mu \neq 0$ which characterizes the neighborhood of a Hopf bifurcation. The convergence to the steady state is marked by an exponential law of the type

$$\rho(t) - \rho^* \simeq (\rho_0 - \rho^*)e^{-t/\tau}, \tag{14}$$

where τ is the relaxation time described by

$$\tau \propto \mu^\delta, \tag{15}$$

where δ is a relaxation exponent. The achievement of the relaxation time τ is discussed as follows. An initial condition is given along the basin of attraction of the attractor. The dynamics is integrated in time using a 4th order Runge-Kutta algorithm. As soon as the distance from the attractor reaches a threshold smaller than 10^{-8}, the integration is interrupted, the time until that point is registered and another simulation is started for a different value of μ. Figure 5 shows the behavior of τ *vs.* μ. A power law fitting gives $\delta = -0.969(9) \simeq -1$.

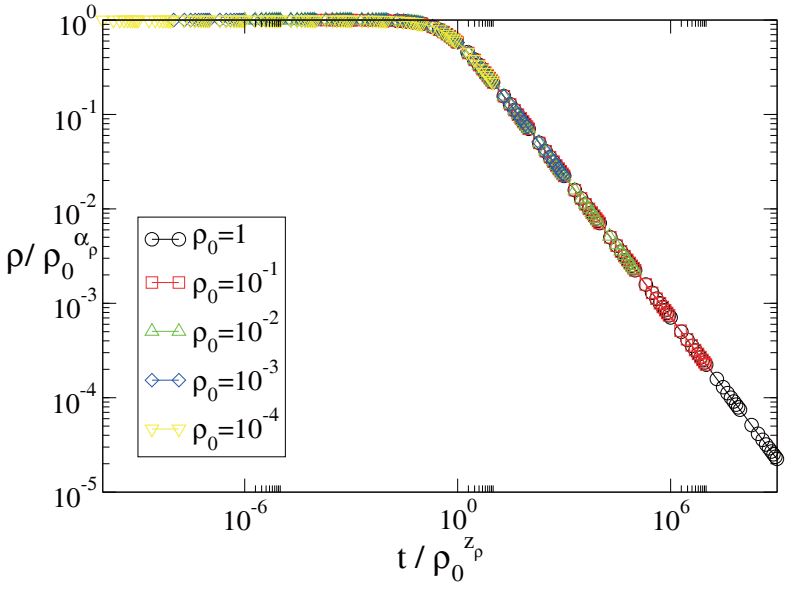

Fig. 4 Overlap of all curves shown in Figure 2 onto a single and universal plot by considering a convenient rescale of the axis.

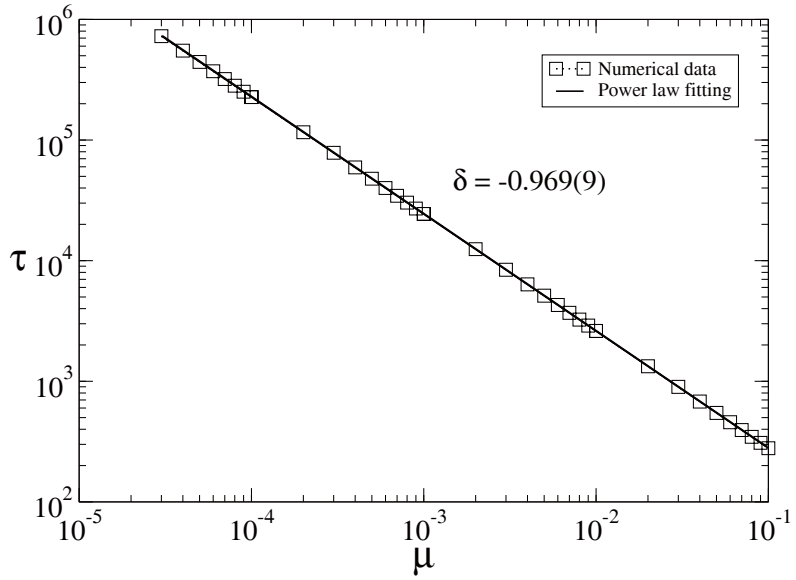

Fig. 5 Plot of the behavior of relaxation time τ against μ. A power law fitting furnishes $\delta = -0.969(9) \simeq -1$.

Let us now discuss the scaling results obtained for the angular equation (see equation (6)). Figure 6 shows the behavior of ϕ *vs.* t for different initial conditions and considering the parameter $\mu = 0$. We see that different initial conditions produce different curves. Depending on the initial value of ϕ_0, the orbits stay in a plateau of constant ϕ for different ranges of time. Moreover after reaching the crossover time, t_x, the orbit changes from a constant regime to a power law growth characterized by the critical exponent β_ϕ. The length of the plateau depends on the initial condition ϕ_0.

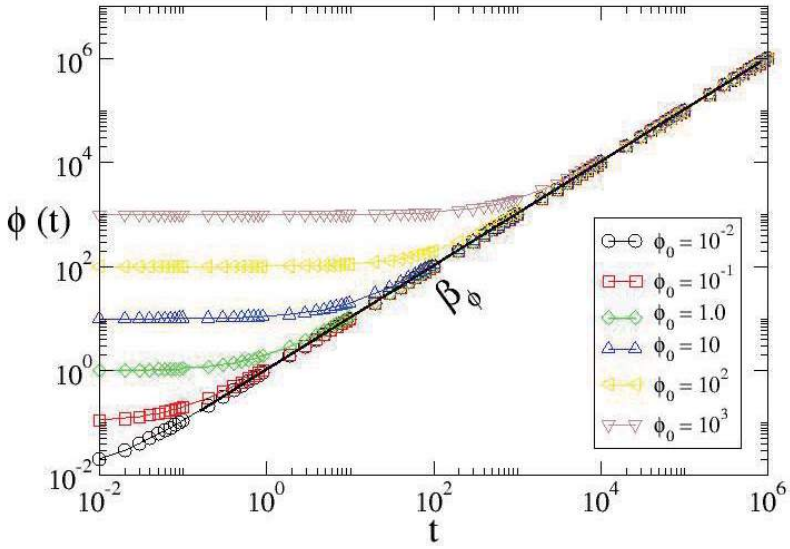

Fig. 6 Plot of the angular variable ϕ as a function of time t for different initial conditions, as labeled in the figure. The parameter used was $\mu = 0$.

This behavior allows us to announce the hypotheses:

1. For $t \ll t_x$, the dynamical variable ϕ behaves as

$$\phi(t) \propto \phi_0^{\alpha_\phi}, \quad t \ll t_x, \tag{16}$$

where from Figure 6 we see easily that $\alpha_\phi = 1$.

2. For large t, typically $t \gg t_x$, the dynamics is as follows

$$\phi(t) \propto t^{\beta_\phi}, \quad t \gg t_x. \tag{17}$$

3. The characteristic crossover time t_x that describes the changeover from a constant regime to a power law growth is given by

$$t_x \propto {\phi_0}^{z_\phi}, \tag{18}$$

where z_ϕ gives the changeover exponent.

The exponents z_ϕ and β_ϕ are obtained by their specific plots. After the constant plateau, a power law fitting gives $\beta_\phi = 0.996(1) \simeq 1$. To obtain the exponent z_ϕ we need to analyze the behavior of t_x *vs.* ϕ_0, see Figure 7. The slope obtained for t_x *vs.* ϕ_0 is $z_\phi = 1.00383(5) \simeq 1$. These scaling hypotheses lead to the same scaling law as discussed before, therefore we obtain that $z_\phi = \alpha_\phi/\beta_\phi$. When the dynamical variables are scaled as $\phi \to \phi/\phi_0^{\alpha_\phi}$ and $t \to t/\phi_0^{z_\phi}$, all curves of $\phi(t)$ *vs.* t are overlapped into a single and universal curve, see figure 8. The dynamics of ϕ *vs.* t for $\mu \neq 0$ is remarkable similar to the results obtained above. In the next section, we discuss the convergence to the steady state for a Hopf bifurcation by considering an analytical approach that involves solving the differentials equations (5) and (6) for both $\mu = 0$ and $\mu \neq 0$.

4 An analytical approach to the steady state for the Hopf Bifurcation

Let us now apply the scale formalism to explore the Hopf bifurcation considering the solution of the differential equations (5) and (6). We start with considering the evolution towards the fixed point at the bifurcation point

$\mu = 0$. The differential equation is then written as

$$\frac{d\rho}{dt} = -\rho^3. \tag{19}$$

A straightforward integration gives

$$\rho(t) = \frac{\rho_0}{\sqrt{1+2t\rho_0^2}}. \tag{20}$$

Let now discuss the implications of equation (20) for specific ranges of t. Considering the case where $2t\rho_0^2 \ll 1$, which is equal to $t \ll t_x$, we realize that $\rho(t) \propto \rho_0$. Therefore, according to the first scaling hypothesis for the radial coordinate we can say the critical exponent $\alpha_\rho = 1$. However, in the case $2t\rho_0^2 \gg 1$ that corresponds to $t \gg t_x$ we get

$$\rho(t) \propto t^{-1/2}. \tag{21}$$

A quick comparison with the second scaling hypothesis of the previous section tell us that $\beta_\rho = -1/2$. The last case is when $2t\rho_0^2 = 1$, which is the case of $t = t_x$. Then we end up with

$$t_x \propto \rho_0^{-2}. \tag{22}$$

Finally, according to third scale hypothesis, we can say that $z_\rho = -2$. These results reinforce our phenomenological approach as discussed in the earlier sections. We then discuss the case of $\mu \neq 0$, therefore considering the convergence to the steady state at a neighborhood of a Hopf bifurcation. We have to solve the following differential equation $\frac{d\rho}{dt} = \mu\rho - \rho^3$. A direct integration gives

$$\rho(t) - \sqrt{\mu} \simeq \frac{\sqrt{\mu}}{2} e^{-2\mu t}. \tag{23}$$

Comparing this result with equations (14) and (15) we get that the relaxation exponent $\delta = -1$. Thus, the results obtained in this section by considering an analytical approach are in complete agreement with the numerical results shown in previous section.

A next step is to investigate the angular equation. We consider first the case of $\mu = 0$. The differential equation, when incorporated the solution of $\rho(t)$ is written as $\frac{d\phi}{dt} = w_0 + b\frac{\rho_0^2}{1+2t\rho_0^2}$. After integration we obtain the following

$$\phi(t) = \phi_0 + w_0 t + \frac{b}{2}\ln(1+2t\rho_0^2). \tag{24}$$

Let now discuss the implications of equation (24) for specific ranges of t. Considering the case where $w_0 t + \frac{b}{2}\ln(1+2t\rho_0^2) \ll \phi_0$, which is equal to $t \ll t_x$, we realize that $\phi(t) \propto \phi_0$ leading to $\alpha_\phi = 1$. However, in the case $w_0 t \gg \phi_0 + \frac{b}{2}\ln(1+2t\rho_0^2)$ that corresponds to $t \gg t_x$ we get $\phi(t) \propto t$, giving $\beta_\phi = 1$. The last case is obtained when $w_0 t = \phi_0 + \frac{b}{2}\ln(1+2t\rho_0^2) \cong \phi_0$, which is the case of $t = t_x$. Then we end up with $t_x \propto \phi_0$, leading to $z_\phi = 1$. This approximation is valid since the function $\ln(t)$ varies slowly as compared to the linear term t.

5 Discussions and conclusions

In a recent result involving bifurcation in 1-D mappings, it was considered particularly a family of logistic-like mappings [26]. The convergence to the fixed point at a bifurcation was investigated using both the phenomenological approach, using a scaling function and obtained at the end a scaling law with three critical exponents as well as an analytical procedure, transforming the equation of differences in a differential equation; later on integrating it easily. The phenomenological investigation considered, as made here, a set of three scaling hypotheses and specific plots to get the critical exponents. It was proved there [26] the exponent $\alpha = 1$ is a constant while

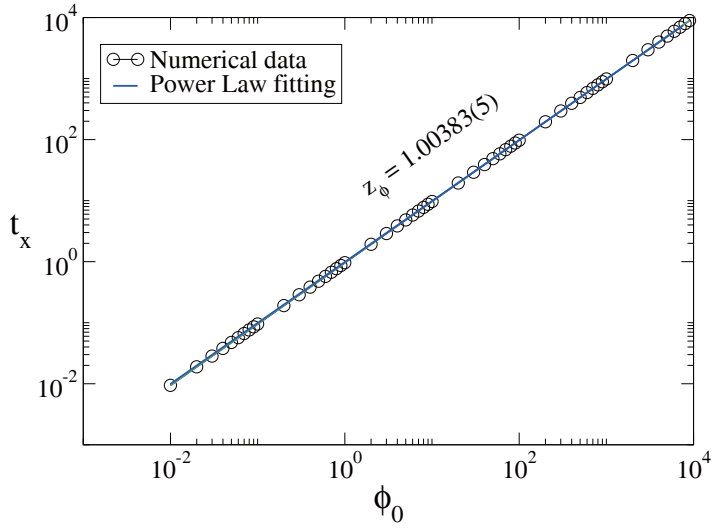

Fig. 7 Plot of the crossover time t_x against the initial condition ϕ_0 together with its power law fitting for $\mu = 0$ with slope $z_\phi = 1.00383(5)$.

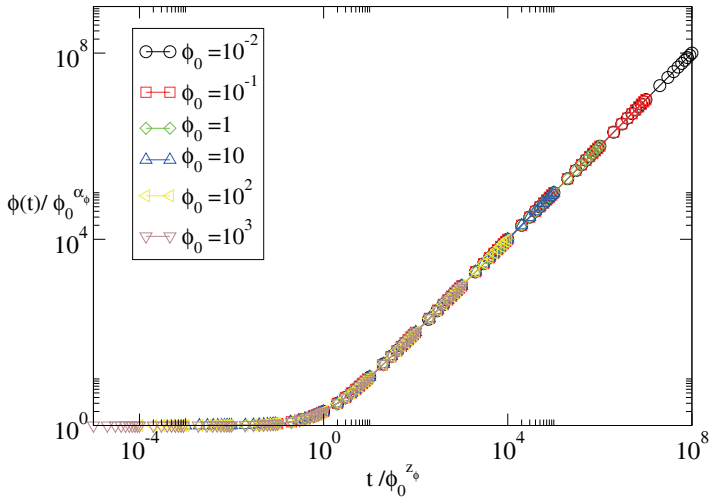

Fig. 8 Overlap of all curves shown in Figure 6 onto a single and therefore universal plot by considering the following transformations: $\phi \to \phi/\phi_0^{\alpha_\phi}$ and $t \to t/\phi_0^{z_\phi}$.

$\beta = -1/\gamma$ and $z = -\gamma$ do depend on the nonlinearity of the mapping. The authors show that for a logistic-like map of the type $x_{n+1} = Rx_n(1-x_n^\gamma)$, where $\gamma \geq 1$ the scaling law $z = \alpha/\beta$ is also observed.

Soon after [26], the authors made a Taylor expansion of the second iterated of the mapping and described with success [27] the critical exponents for a period doubling bifurcation. For this bifurcation, the exponents do not depend on the nonlinearity of the mapping and are then universal: $\alpha = 1$, $\beta = -1/2$ and $z = -2$. As discussed in Refs. [26, 27] the critical exponents are packed in Table 1.

An extension of the procedure was made also for a set of bifurcations observed in ordinary differential equations (see Ref. [28]) considering a set of three important bifurcations of 1-D flow namely: saddle-node, transcritical and supercritical pitchfork. The results are summarized in Table 2.

In the present paper, our results extend the formalism to be used in a Hopf bifurcation. Because after the bifurcation the attractor is a limit cycle in a plane, it turns out to be convenient to use polar coordinate to investigate the dynamics. Instead of a single set of critical exponent, the dynamics needs two sets, among the

Table 1 Table of critical exponents α, β, z and δ observed for a family of logistic-like map $x_{n+1} = Rx_n(1-x_n^{\gamma})$, as discussed in Refs. [26, 27].

Bifurcation	α	β	z	δ
Pitchfork	1	$-\frac{1}{\gamma}$	$-\gamma$	-1
Transcritical	1	$-\frac{1}{\gamma}$	$-\gamma$	-1
Period doubling	1	$-\frac{1}{2}$	-2	-1

Table 2 Table of critical exponents α, β, z and δ for the three bifurcations discussed in Ref [28].

Equation	Bifurcation	α	β	z	δ
$\dot{x} = \mu - x^2$	Saddle-node	1	-1	-1	$-\frac{1}{2}$
$\dot{x} = \mu x - x^2$	Transcritical	1	-1	-1	-1
$\dot{x} = \mu x - x^3$	Supercritical pitchfork	1	$-\frac{1}{2}$	-2	-1

Table 3 Table of critical exponents $\alpha_{\rho,\phi}$, $\beta_{\rho,\phi}$, $z_{\rho,\phi}$ and δ for a Hopf bifurcation.

	Radial	Angular
α	1	1
β	$-1/2$	1
z	-2	1
δ	-1	–

exponent δ. One set describes the convergence in the radial coordinate while the other set describes the evolution of the angular variable. Our results can be compacted as shown in Table 3.

The results discussed here allow to understand the scaling properties of dynamical variable at and near at a Hopf bifurcation. Our results can be an alternative form to investigate and classify the type of bifurcation in experimental systems, e.g., electrical circuits, when the set of equations describing the dynamics are not all known. Presently we are working in a Chua circuit to investigate such properties experimentally.

Acknowledgements

V.B.S. thanks to FAPESP (2015/23142-0). E.D.L acknowledges support from FAPESP (2012/23688-5) and CNPq (303707/2015-1) Brazilian agencies.

Appendix: Proof of Lemma 1

Proof. In this appendix we discuss the proof of lemma 1. This proof is remarkably similar to the Kuznetsov's procedure made in [29]. Writing equations (1) and (2) into the complex form, we have

$$\dot{z} = z(\mu + iw_0) + |z|\, z^2(a+ib) + \cdots, \tag{25}$$

and while truncating the higher order terms we obtain

$$\dot{z} = z(\mu + iw_0) + |z|\, z^2(a+ib). \tag{26}$$

Our objective is to prove that equation (25) is locally topologically equivalent near to the origin to equation (26). To do that we suppose:

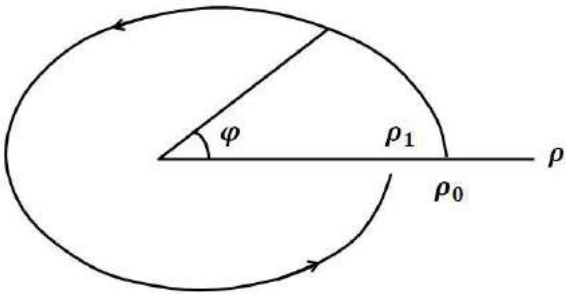

Fig. 9 The Poincaré (return) map near Hopf Bifurcation (Source: Kuznetsov, 1998, p. 109).

Step 1 (existence and uniqueness of the limit cycle). Writing the equation (25) in polar coordinates (ρ,ϕ) with $z=\rho e^{i\phi}$ we end up with

$$\frac{d\rho}{dt}=\rho(\mu+a\rho^2)+\Phi(\rho,\phi),$$
$$\frac{d\phi}{dt}=w_0+\Psi(\rho,\phi),$$

where Φ and Ψ are smooth functions of (ρ,ϕ,μ). The terms Φ and Ψ incorporate the higher order terms of the equation (25). Once both a and w_0 are constants we can fix them as $a=-1$ and $w_0=1$. This gives

$$\frac{d\rho}{dt}=\rho(\mu-\rho^2)+\Phi(\rho,\phi), \tag{27}$$
$$\frac{d\phi}{dt}=1+\Psi(\rho,\phi). \tag{28}$$

For a given μ, an orbit of the system described by equations (27) and (28) starting from $(\rho,\phi)=(\rho_0,0)$ has a typical representation as shown in figure 9 where $\rho=\rho(\phi,\rho_0)$, $\rho(0,\rho_0)=\rho_0$ with ρ satisfying the equation

$$\frac{d\rho}{d\phi}=\frac{\rho(\mu-\rho^2)+R(\rho,\phi)}{1+\Psi(\rho,\phi)}=\rho(\mu-\rho^2)+R(\rho,\phi), \tag{29}$$

where $R(\rho,\phi)$ is a smooth function that incorporates the higher order terms. Since $\rho(\phi,0)\equiv 0$ we have

$$\frac{d\rho}{d\phi}(\rho,0)=\frac{d^2\rho}{d\rho d\phi}(\rho,0)=\frac{d^2\rho}{d\phi^2}(\rho,0)=\cdots=0. \tag{30}$$

A Taylor series expansion of $\rho(\phi,\rho_0)$ is written as

$$\rho(\phi,\rho_0)=u_1(\phi)\rho_0+u_2(\phi)\rho_0^2+u_3(\phi)\rho_0^3+\ldots, \tag{31}$$

where

$$u_1(\phi)=\frac{d\rho}{d\rho_0}\Big|_{\rho_0=0},u_2(\phi)=\frac{1}{2!}\frac{d^2\rho}{d\rho_0^2}\Big|_{\rho_0=0},u_3(\phi)=\frac{1}{3!}\frac{d^3\rho}{d\rho_0^3}\Big|_{\rho_0=0},\ldots \tag{32}$$

Substituting equations (32) in (31) and sorting terms according to power of ρ_0, we arrive in the following linear differential equations

$$\frac{du_1(\phi)}{d\phi}=\mu u_1(\phi),$$
$$\frac{du_2(\phi)}{d\phi}=\mu u_2(\phi),$$
$$\frac{du_3(\phi)}{d\phi}=\mu u_3(\phi)-u_1(\phi)^3,$$

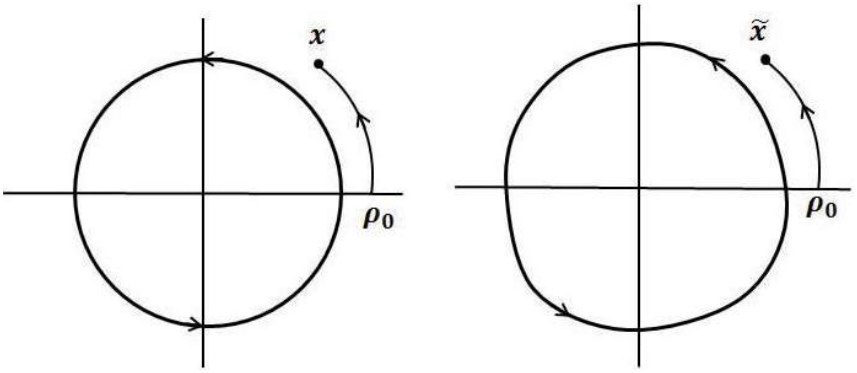

Fig. 10 Construction of the homeomorphism neat the Hopf bifurcation.

with the initial conditions $u_1(0) = 1$, $u_2(0) = u_3(0) = 0$. The solutions for the differential equations above are respectively

$$\begin{aligned} u_1(\phi) &= e^{\mu\phi}, \\ u_2(\phi) &= 0, \\ u_3(\phi) &= \frac{e^{\mu\phi}(1-e^{2\mu\phi})}{2\mu}. \end{aligned}$$

Notice that these expressions are independent of $R(\rho,\phi)$. Thus the Poincaré return map $\rho_0 \rightharpoonup \rho_1 = \rho(2\pi,\rho_0)$ is written as

$$\rho_1 = \rho_0 e^{2\mu\pi} - e^{2\mu\pi}(2\pi + O(\mu))\rho_0^3 + H.O.T., \tag{33}$$

for all smooth $R = H.O.T.$. Now according to Ref. [29] this map can be analyzed for sufficiently small ρ_0 and $|\mu|$ with the Implicit Function Theorem. By the application of the Implicit Function Theorem we can establish there is a neighborhood of the origin in which the map has only the trivial fixed point for small $\mu < 0$ and an additional fixed point, $\rho_0^{(0)} = \sqrt{\mu} + \ldots$, for small $\mu > 0$. Taking into account that a positive fixed point of the map corresponds to a limit cycle of the system, we can infer that equations (27) and (28) with any higher-order terms have a unique (stable) limit cycle bifurcating from the origin and existing for $\mu > 0$ just as equation (26). Therefore, the higher-order terms do not affect the limit cycle bifurcation in some neighborhood of $z = 0$ for $|\mu|$ sufficiently small.

Step 2 (Construction of a homeomorphism). Now we have to prove that the phase portrait of equations (1) and (2) are topologically equivalent to that one obtained from equations (3) and (4). In order to do so, we establish a small but positive μ. From the step 1 we verified the systems (25) and (26) both have a limit cycle in some neighborhood of the origin. Notice that the transition from equation (28) to (31) is equivalent to the introduction of a new time re-parametrization such that the return time to the half-axis $\phi = 0 \pmod{2\pi}$ is the same for all orbits starting on this axis with $\rho_0 > 0$. Next, we apply a linear scaling of ρ-coordinate of the system (28) such that the point of intersection of the cycle and the horizontal half-axis be at $\rho = \sqrt{\mu}$.

We now define a map $\widetilde{x} \rightharpoonup x$ by the following construction (see Ref. [29] for further details). Take a point $x = (x,y)$ and find values (ρ_0,τ_0), where τ_0 is the minimal time required for an orbit of equation (26) to approach the point x starting from the horizontal half-axis with $\rho = \rho_0$ and construct an orbit of the system (25) on the time interval $[0,\tau_0]$ starting at this point. Denote the resulting point by $\widetilde{x} = (\widetilde{x},\widetilde{y})$ (see figure 10). Set $\widetilde{x} = 0$ for $x = 0$. In this way the map constructed is a homeomorphism that, for $\mu > 0$, maps orbits of system (26) in some neighborhood of the origin into orbits of (25) preserving time direction.

References

[1] Strogatz, S.H. (2015), *Nonlinear dynamics and chaos: with applications to physics, biology, chemistry and engineering,* Westview Press.

[2] Bashkirtseva, I. and Ryashko, L. (2011), Sensitivity analysis of stochastic attractors and noise-induced transitions for population model with Allee effect, *Chaos*, **21**, 047514.

[3] Strogatz, S.H. (2000), From Kuramoto to Crawford: exploring the onset of synchronization in populations of coupled oscillators, *Physica D: Nonlinear Phenomena*, **143**, 1.

[4] Georgiou, I.T. and Romeo, F. (2015), Multi-physics dynamics of a mechanical oscillator coupled to an electro-magnetic circuit, *Int. J. Nonlinear. Mech.*, **70**, 153.

[5] Gardine, L., Fournier-Prunaret, D., and Charge, P. (2011), Border collision bifurcations in a Two-dimensional PWS map from a simple circuit, *Chaos*, **21**, 023106.

[6] Inarrea, M., Palacian, J.F., and Pascual, A.I. (2011), Bifurcations of dividing surfaces in chemical reactions, *J. Chem. Phys*., **135**, 014110.

[7] Bakes, D., Schreiberova, L., and Schreiber, I. (2008), Mixed-mode oscillations in a homogeneous pH-oscillatory chemical reaction system, *Chaos* **18**, 015102.

[8] Guckenheimer, J. (2008), Return maps of folded nodes and folded saddle-nodes, *Chaos*, **18**, 015108.

[9] Philominathan, P., Santhiah, M., Mohamed, IR., Murali, K., and Rajasekar, S. (2011), Chaotic dynamics of a simple parametrically driven dissipative circuit, *Int. J. Bifurcations and Chaos*, **21**, 1927.

[10] Virte, M., Panajotov, K., and Thienpont, H. (2013), Deterministic polarization chaos from a laser diode, *Nat. Photonics*, **7**, 60.

[11] Doedel, EJ. and Pando-L, CL. (2011), Isolas of periodic passive Q-switching self-pulsations in the three-level:two-level model for a laser with a saturable absorber, *Phys. Rev. E.*, **84**, 056207.

[12] Cavalcante, H.L.D.S. and Leite-Rios, J.R. (2008), Experimental bifurcations and homoclinic chaos in a laser with a saturable absorber, *Chaos*, **18**, 023107.

[13] Guo, Y. and Luo, A.C.J. (2012), Parametric analysis of bifurcation and chaos in a periodically driven horizontal impact, *Int. J. Bifurc. Chaos*, **22**, 1250268.

[14] Luo, A.C.J. and O'Connor, D. (2009), Periodic motions and chaos with impacting chatter with stick in a gear transmission system, *Int. J. Bifurc. Chaos*, **19**, 2093.

[15] Yang, J.H., Sanjuan, M.A.F., Liu, H.G., and Cheng G. (2015), Bifurcation Transition and Nonlinear Response in a Fractional-Order System, *J. Comput. Nonlinear. Dyn.*, **10**, 061017.

[16] Grebogi, C., Ott, E., and Yorke, J.A. (1983), Chaotic attractors in crisis, *Phys. Rev. Lett.*, **48**, 1507.

[17] Grebogi, C., Ott, E., and Yorke, J.A. (1983), Crises, sudden changes in chaotic attractors, and trasient chaos, *Physica D*, **7**, 181.

[18] Leonel, E.D. and McClintock, P.V.E. (2005), A crisis in the dissipative Fermi accelerator model, *J. Phys. A: Math. Gen*, **38**, L425.

[19] Oliveira, D.F.M., Leonel, E.D., and Robnik, M. (2011), Boundary crisis and transient in a dissipative relativistic standard map, *Phys. Lett. A*, **375**, 3365.

[20] Helrich, C.S. (2009), *Modern thermodynamics with statistical mechanics*, Heidelberg: Springer-Verlag.

[21] Reif, F. (1965), *Fundamentals of statistical and thermal physics*, New York: McGraw-Hill.

[22] Pottier, N. (2010), *Nonequilibrium statistical physics, linear irreversible processes*, Oxford: Oxford University Press.

[23] Cardy, J. (1996), Scaling and renormalization in statistical physics, Cambridge: Cambridge University Press.

[24] Kadanoff, L.P. (1999), *Statistical physics: statics, dynamics and renormalization*, Singapore: World Scientific.

[25] Leonel, E.D., da Silva, J.K.I., and Kamphorst, S.O. (2002), Relaxation and transients in a time-dependent logistic map, *Int. J. Bifurc. Chaos*, **12**, 1667.

[26] Teixeira, R.M.N., Rando, D.S., Geraldo, F.C., Costa Filho, R.N., Oliveira, J.A., and Leonel, E.D. (2015), Convergence towards asymptotic state 1-D mappings: A scaling investigation, *Phys. Lett. A*, **379**, 1246

[27] Teixeira, R.M.N., Rando, D.S., Geraldo, F.C., Costa Filho, R.N., Oliveira, J.A., and Leonel, E.D. (2015), Addendum to: "Convergence towards asymptotic state 1-D mappings: A scaling investigation", *Phys. Lett. A*, **379**, 1246, 1796.

[28] Leonel, E.D. (2016), Defining universality classes for three different local bifurcations, *Commun. Nonlinear Sci. Numer. Simulat.*, **39**, 520.

[29] Kuznetsov, Y.A. (1998), *Elements of applied bifurcation theory*, New York: Springer Science & Business Media, **112**.